Rydberg states of the hydrogen-antihydrogen quasimolecule

V. Sharipov,[1] L. Labzowsky,[1,2,3] and G. Plunien[4]
[1]*Institute of Physics, St. Petersburg State University, 198904, Uljanovskaya 1, Petrodvorets, St. Petersburg, Russia*
[2]*Petersburg Nuclear Physics Institute, 188350, Gatchina, St. Petersburg, Russia*
[3]*Max-Planck Institut für Physik komplexer Systeme, Nöthnitzerstrasse 38, D-01187 Dresden, Germany*
[4]*Technische Universität Dresden, Mommsenstrasse 13, D-01062, Dresden, Germany*
(Received 28 December 2005; published 11 May 2006)

A description of the excited lepton states of the hydrogen-antihydrogen quasimolecule is presented. Potential energy curves and the leptonic part of the wave functions corresponding to a variety of such states are calculated within the Born-Oppenheimer approximation employing the Ritz variational principle. Nonadiabatic corrections to the leptonic potentials are also obtained. Basis functions are constructed as products of explicitly correlated Gaussians and spherical harmonics which describe correctly the motion of leptons with arbitrary orbital angular momentum projection onto the molecular (internuclear) axis. The hadronic part of the wave function for each leptonic level of the hydrogen-antihydrogen system is calculated by solving the Schrödinger equation with the obtained leptonic potentials. Corresponding solutions are generated utilizing precise B-spline representations. Employing leptonic and hadronic parts of the wave function the electron-positron and proton-antiproton annihilation rates are computed for a number of quasimolecular states. The decay rates of the hydrogen-antihydrogen system into separate positronium and protonium atoms are also estimated for the quasimolecular levels under consideration.

DOI: 10.1103/PhysRevA.73.052503 PACS number(s): 36.10.−k, 31.30.Jv, 12.20.Ds, 31.15.−p

I. INTRODUCTION

Recent experimental success in the production of antihydrogen atoms [1–3] has raised interest in the interaction between atoms and antiatoms. The simplest atom-antiatom (hydrogen-antihydrogen) system has been the subject of studies for decades [4]. The general behavior of the potential energy curve of the ground state of the hydrogen-antihydrogen ($H\bar{H}$) system has been established in [4] and has been recently calculated with high accuracy [5]. The interaction between helium and antihydrogen atoms has also been investigated [6,7], and a small potential barrier was predicted in this system. Most calculations concerning the $H\bar{H}$ interaction have been performed within the Born-Oppenheimer approximation employing variational methods. Nonadiabatic corrections also have been estimated in [7–9]. Both scattering phenomena and quasibound molecular states of $H\bar{H}$ system have been considered in [10–12] and [9]. Cross sections for the processes occurring in H-$\bar{H}$ scattering—i.e., (i) the rearrangement, when the $H\bar{H}$ system transforms into positronium (Ps) and protonium (Pt), (ii) leptonic, and (iii) hadronic annihilation—have been calculated and compared with each other [13]. The corresponding decay processes for a number of quasibound $H\bar{H}$ molecular states were calculated in [9]. Such quasibound states can arise via three-body interactions, including one extra atom or via radiative association [14]. As has been pointed out in [4] a critical internuclear distance (R_c) exists at which the $H\bar{H}$ system transforms into a Ps atom weakly interacting with the proton (p^+) and the antiproton (p^-), respectively. The decay $H\bar{H} \rightarrow \mathrm{Ps}+\mathrm{Pt}$ and hadronic annihilation decay were found to be the leading processes. For the collision scenario the corresponding decay rates are comparable [13], while for quasimolecular states with high quantum numbers the hadronic annihilation rates are somewhat larger than for the $H\bar{H} \rightarrow \mathrm{Ps}+\mathrm{Pt}$ decay rates [9]. The leptonic annihilation process is negligible in both cases.

So far all calculations concerning the H-$\bar{H}$ interaction have been performed for the leptonic ground state of this system. However, in experiments the $\bar{H}$ atoms are produced in Rydberg states [3]. Accordingly, the $H\bar{H}$ system will be predominantly formed in excited states with high values of leptonic orbital angular momentum projection and therefore it is important to investigate the potential energy curves, leptonic and hadronic annihilation rates, and $H\bar{H}^* \rightarrow \mathrm{Ps}+\mathrm{Pt}$ decay rates of the $H\bar{H}^*$ quasimolecule for leptonic Rydberg levels.

In the present paper the description of excited state of the $H\bar{H}^*$ system with arbitrary leptonic orbital angular momentum projection Λ onto the internuclear axis is given. This description is based on a precise solution of the few-body problem by means of the stochastic variational method dealing with a correlated Gaussian basis as has been developed in [15,16]. Within the framework of this method p^-p^+ and e^-e^+ annihilation rates, critical internuclear distances $R_c(\Lambda)$, and $H\bar{H}^* \rightarrow \mathrm{Ps}+\mathrm{Pt}$ decay rates have been calculated for a number of quasibound hadronic states. Atomic units will be used throughout this paper.

The paper is organized as follows. In Sec. II on the basis of the Born-Oppenheimer approximation we solve the equation for leptons for every fixed position of hadrons, thus defining the potential curves for different leptonic orbital angular momentum projections. In the same section we solve also the Schrödinger equation for the hadron movement with a certain potential curve. The results for the potential curves and their properties are discussed in Sec. III. In Sec. IV we

evaluate decay rates for the unstable $H\bar{H}$ system, corresponding to the transition to Ps+Pt atoms. Section V is devoted to the calculation of the leptonic and hadronic annihilation rates. Section VI contains conclusions, including a comparison of importance of various decay channels and a possible connection to modern experiments. In the Appendix the details of the applied mathematical and computational methods are given.

II. DESCRIPTION OF THE $H\bar{H}$ SYSTEM IN EXCITED STATE

We consider the $H\bar{H}$ system within the Born-Oppenheimer approximation. This means that the four-particle wave function $\Psi(\vec{r}_{e^-},\vec{r}_{e^+},\vec{R})$ is represented by the product

$$\Psi(\vec{r}_{e^-},\vec{r}_{e^+},\vec{R}) = \Psi^{lep}(\vec{r}_{e^-},\vec{r}_{e^+},\vec{R})\Psi^{had}(\vec{R}), \tag{1}$$

where $\vec{r}_{e^-}$ and $\vec{r}_{e^+}$ are the position vectors of the electron and the positron with respect to the center-of-mass system, $R=|\vec{R}|$ denotes the internuclear distance, where $\vec{R}$ is directed from the H to the $\bar{H}$ atom. The spin parts of the leptonic and hadronic wave functions are not considered in the further discussion. The only difference between $^1\Lambda$ and $^3\Lambda$ states arises for the electron-positron annihilation process (see Sec. V). However, the role of this process is negligible compared to that of the hadron annihilation and the $H\bar{H}^* \rightarrow$ Ps+Pt decay channel.

The leptonic wave function $\Psi^{lep}(\vec{r}_{e^-},\vec{r}_{e^+},\vec{R})$ and the hadronic wave function $\Psi^{had}(\vec{R})$ satisfy the corresponding Schrödinger equations. For the leptonic part it takes the form

$$\hat{H}^{lep}(\vec{r}_{e^-},\vec{r}_{e^+},\vec{R})\Psi^{lep}_{\Lambda}(\vec{r}_{e^-},\vec{r}_{e^+},\vec{R}) = V^{lep}_{\Lambda}(R)\Psi^{lep}_{\Lambda}(\vec{r}_{e^-},\vec{r}_{e^+},\vec{R}), \tag{2}$$

$$\hat{H}^{lep}(\vec{r}_{e^-},\vec{r}_{e^+},\vec{R}) = -\frac{1}{2}\nabla^2_{e^-} - \frac{1}{2}\nabla^2_{e^+} - \frac{1}{\left|\vec{r}_{e^-}+\frac{1}{2}\vec{R}\right|} - \frac{1}{\left|\vec{r}_{e^+}-\frac{1}{2}\vec{R}\right|} + \frac{1}{\left|\vec{r}_{e^-}-\frac{1}{2}\vec{R}\right|} + \frac{1}{\left|\vec{r}_{e^+}+\frac{1}{2}\vec{R}\right|} - \frac{1}{|\vec{r}_{e^-}-\vec{r}_{e^+}|}. \tag{3}$$

The equation of motion for the hadronic part of the wave function reads

$$\left(-\frac{1}{m_p}\nabla^2_{\vec{R}} + V^{lep}_{\Lambda}(R) - \frac{1}{R}\right)\Psi^{had}_{\Lambda nlm}(\vec{R}) = E_{\Lambda nl}\Psi^{had}_{\Lambda nlm}(\vec{R}), \tag{4}$$

where $m_p=1836.15$ a.u. is the proton mass. For the description of the hadronic motion we use the set of quantum numbers Λnlm. The quantum number Λ defines the leptonic term, which corresponds to a certain potential $V^{lep}_{\Lambda}(R)$. The quantum numbers nlm correspond to the standard set of quantum numbers for the particle motion in the central field or for the two-particle problem in the center-of-mass reference frame. In ordinary diatomics the vibrational v and rotational J quantum numbers are commonly used for a description of hadronic motion. The quantum number J denotes the total angular momentum of the molecule, including leptonic and hadronic contributions. In case of the nonclosed leptonic shells it should contain also the leptonic spin part. For the unstable quasimolecular states in the $H\bar{H}^*$ system the use of the quantum numbers vJ is not so easy. The employment of the set nl, where l denotes the pure hadronic orbital angular momentum, has some advantages in case of the $H\bar{H}^*$ system. The main advantage is that below the critical distance $R_c(\Lambda)$ the $H\bar{H}^*$ system transforms to Pt+Ps systems. Then the quantum numbers nl become the standard hydrogenic-type numbers for the Pt atom.

The leptonic potential $V^{lep}_{\Lambda}(R)$ defined in Eq. (2) is shifted by the value $E^{bind}_{1s}(H)+E^{bind}_{\Lambda+1}(\bar{H})$ so that $V^{lep}_{\Lambda}(R)\rightarrow 0$ holds in the limit $R\rightarrow\infty$. This shifted potential enters the Schrödinger equation for hadrons [Eq. (4)]. Here $E^{bind}_{1s}(H)$ and $E^{bind}_{\Lambda+1}(\bar{H})$ are the binding energies of the hydrogen atom in the ground state and the antihydrogen atom in an excited state with principal quantum number, equal to $\Lambda+1$, respectively. This corresponds to a particular choice of Rydberg states of the antihydrogen atom—namely, those Rydberg states with positron orbital angular momentum quantum numbers $l_{e^+}=n_{e^+}-1$, where n_{e^+} is the principal quantum number. It can be argued that such states should arise predominantly in the experiments. Indeed, if the Rydberg state for a certain n_{e^+} value ($n_{e^+}\sim 30$ in [3]) is fixed by experimental conditions, then the mean radial position $\bar{r}_{e^+}$ of the positron in the corresponding orbit will be of the order $n^2_{e^+}$ a.u. The cross section for positron capture by the cold antiproton should have a maximum when the kinetic energy of the positron in the antiproton frame of reference will be of order $n^{-2}_{e^+}$ a.u. Consequently, the positron momentum $\bar{p}_{e^+}$ will be of order $n^{-1}_{e^+}$ a.u., and the absolute value of the positron orbital angular momentum will scale as $\bar{l}_{e^+}\approx\bar{r}_{e^+}\bar{p}_{e^+}\approx n_{e^+}$ a.u.

At very large internuclear distances R the wave function $\Psi^{lep}_{\Lambda}(\vec{r}_{e^-},\vec{r}_{e^+},\vec{R})$ is taken in the form of a product of wave functions describing a free hydrogen atom in the ground state and free antihydrogen atom in the excited state:

$$\Psi^{lep}_{\Lambda}(\vec{r}_{e^-},\vec{r}_{e^+},\vec{R}) = \Psi_{100}(\vec{r}_{e^-}+\vec{R}/2)\Psi_{\Lambda+1\Lambda\Lambda}(\vec{r}_{e^+}-\vec{R}/2). \tag{5}$$

This asymptotic of $\Psi^{lep}_{\Lambda}(\vec{r}_{e^-},\vec{r}_{e^+},\vec{R})$ defines the leptonic state under consideration. Accordingly, we started our variational calculations for the leptonic wave function from the value $R=20$ a.u. which still can be considered as an asymptotic region. The interaction energy between H and $\bar{H}^*$ atoms, which is equal to

$$E_{\Lambda}(R) = V^{lep}_{\Lambda}(R) - 1/R, \tag{6}$$

defines the potential energy curve for the excited leptonic state.

The wave function of light particles $\Psi^{lep}_{\Lambda}(\vec{r}_{e^-},\vec{r}_{e^+},\vec{R})$ describes the motion of electron and positron in the field of a p^-p^+ pair, fixed at distance R. The nonadiabatic correction is

defined by the derivative $\frac{\partial \Psi_{\Lambda}^{lep}(\vec{r}_{e^-},\vec{r}_{e^+},\vec{R})}{\partial R}$. Letting $\Psi_{\Lambda}^{lep}(\vec{r}_{e^-},\vec{r}_{e^+},\vec{R})$ be normalized according to

$$\int\int d\vec{r}_{e^-}d\vec{r}_{e^+}|\Psi_{\Lambda}^{lep}(\vec{r}_{e^-},\vec{r}_{e^+},\vec{R})|^2 = 1, \tag{7}$$

the nonadiabatic correction $\Delta V_{\Lambda}^{lep}(R)$ takes the form

$$\Delta V_{\Lambda}^{lep}(R) = \frac{1}{m_p}\int\int d\vec{r}_{e^-}d\vec{r}_{e^+}\left|\frac{\partial \Psi_{\Lambda}^{lep}(\vec{r}_{e^-},\vec{r}_{e^+},\vec{R})}{\partial R}\right|^2. \tag{8}$$

The values of $\Delta V_{\Lambda}^{lep}(R)$ have been calculated within the Born-Handy method [17]. It has been pointed out that $\Delta V_{\Lambda}^{lep}(R)$ becomes comparable to the value of $V_{\Lambda}^{lep}(R)$ near the critical distance $R_c(\Lambda)$, where the $H\bar{H}$ system is supposed to transform into the positronium and protonium [8,9] (see also Table II). This means that the Born-Oppenheimer approximation breaks down near $R_c(\Lambda)$.

Since the potential generated by fixed hadrons has the axial symmetry, the electron-positron states are characterized by the value of the leptonic orbital angular momentum projection Λ onto the internuclear axis $\vec{R}$:

$$\hat{L}_{\vec{R}}\Psi_{\Lambda}^{lep}(\vec{r}_{e^-},\vec{r}_{e^+},\vec{R}) = \Lambda\Psi_{\Lambda}^{lep}(\vec{r}_{e^-},\vec{r}_{e^+},\vec{R}), \tag{9}$$

$$\hat{L}_{\vec{R}} = i\left(\frac{\partial}{\partial\varphi_{e^-}} + \frac{\partial}{\partial\varphi_{e^+}}\right), \tag{10}$$

where $\hat{L}_{\vec{R}}$ is the leptonic orbital angular momentum projection operator and φ_{e^-} and φ_{e^+} are the azimuthal coordinates of the electron and the positron, respectively.

The wave function of hadrons $\Psi_{\Lambda nlm}^{had}(\vec{R})$ describes the motion of p^- and p^+ in the effective potential $V_{\Lambda}^{lep}(R)$ created by the leptons together with the attractive Coulomb potential between the proton and antiproton. The energies $E_{\Lambda nl}$ defined in Eq. (4) are the energies of quasimolecular levels corresponding to the leptonic states with the projection of orbital angular momentum equal to Λ. The formation of such states under the experimental conditions corresponding to [1–3] has been discussed in [9].

The leptonic wave function $\Psi_{\Lambda}^{lep}(\vec{r}_{e^-},\vec{r}_{e^+},\vec{R})$ can be represented as the sum of explicitly correlated Gaussians (ECG's) multiplied by the spherical functions:

$$\Psi_{\Lambda}^{lep}(\vec{r}_{e^-},\vec{r}_{e^+},\vec{R}) = \sum_{i=1}^{K} C_i\hat{P}\exp[-a_i(\vec{r}_{e^-}-\vec{r}_{e^+})^2]$$

$$\exp[-b_i(\vec{r}_{e^-}-\vec{R}_i^{e^-})^2 - c_i(\vec{r}_{e^+}-\vec{R}_i^{e^+})^2]\eta_{\Lambda}(\vec{v}_i), \tag{11}$$

where $\vec{v}_i = u_i^{e^-}\vec{r}_{e^-} + u_i^{e^+}\vec{r}_{e^+}$ and

$$\eta_{\Lambda}(\vec{v}_i) = |\vec{v}_i|^{\Lambda}Y_{\Lambda\Lambda}(\Omega_{\vec{v}_i}). \tag{12}$$

Here $Y_{\Lambda\Lambda}(\Omega_{\vec{v}})$ is the spherical harmonic, $\Omega_{\vec{v}_i}$ is the angular part of the vector $\vec{v}_i$, and a_i, b_i, c_i, $\vec{R}_i^{e^-}$, $\vec{R}_i^{e^+}$, $u_i^{e^-}$, $u_i^{e^+}$, and C_i are variational parameters. The leptonic wave function does not require antisymmetrization since the electron and positron are distinct particles. The operator $\hat{P}$ ensures the proper symmetry of $\Psi_{\Lambda}^{lep}(\vec{r}_{e^-},\vec{r}_{e^+},\vec{R})$ charge conjugation. This operator exchanges the electron and positron and reflects their coordinates in the plane which is the perpendicular bisector of the internuclear axis [4]. Leptonic states of the $H\bar{H}$ system are characterized by the eigenvalues of $\hat{P}$:

$$\hat{P}\Psi_{\Lambda}^{lep}(\vec{r}_{e^-},\vec{r}_{e^+},\vec{R}) = \pm\Psi_{\Lambda}^{lep}(\vec{r}_{e^-},\vec{r}_{e^+},\vec{R}). \tag{13}$$

In the following we shall focus on even states only. The potential curves of odd states of the $H\bar{H}^*$ system increase monotonically as the internuclear distance decreases and therefore cannot provide any hadronic quasibound states. The wave function defined in Eq. (11) satisfies the condition (9), so it can describe the excited leptonic states with definite orbital angular momentum projection. ECG's are sufficiently flexible to approximate an exact solution $\Psi_{\Lambda}^{lep}(\vec{r}_{e^-},\vec{r}_{e^+},\vec{R})$ of Eq. (2), and many very accurate results concerning normal and positronic matter have been obtained by using the ECG basis set [15,16,18,19]. Expressions for the overlap integral between two ECG's, matrix elements of $\hat{H}^{lep}(\vec{r}_{e^-},\vec{r}_{e^+},\vec{R})$ as defined in Eq. (3), and the matrix element of the spatial delta function $\delta(\vec{r}_{e^-}-\vec{r}_{e^+})$ are presented in the Appendix. In our variational calculations the number of terms in the sum of Eq. (11) was $K=64$. The energy has been minimized for each parameter employing the golden section method.

The obtained leptonic potential was inserted into the Schrödinger equation for the hadron motion [Eq. (4)]. Since $V_{\Lambda}^{lep}(R)$ depends only on $|\vec{R}|$, the variables in Eq. (4) can be separated:

$$\Psi_{\Lambda nlm}^{had}(\vec{R}) = \frac{1}{R}\chi_{\Lambda nl}(R)Y_{lm}(\Omega_{\vec{R}}), \tag{14}$$

where $Y_{lm}(\Omega_{\vec{R}})$ is the spherical function and $\Omega_{\vec{R}}$ denotes the angular part of vector $\vec{R}$. Substitution of Eq. (14) into Eq. (4) yields

$$\frac{d^2\chi_{\Lambda nl}}{dR^2} + \left[m_p\left(E_{\Lambda nl} - V_{\Lambda}^{lep}(R) + \frac{1}{R}\right) - \frac{l(l+1)}{R^2}\right]\chi_{\Lambda nl} = 0. \tag{15}$$

This equation has been solved by means of the B-spline approach [20,21]. We have utilized spline functions of order 9 together with a number of grid points equal to 1000 for generating numerically the level energies $E_{\Lambda nl}$ and the radial functions $\chi_{\Lambda nl}(R)$. Below we shall consider the solutions with $l=0,1$ and $n \gg 1$. The levels with low values of the principal quantum number n correspond most likely to the bound states of Pt atom.

The total energy of the $H\bar{H}^*$ quasimolecule consists of three parts: $E_{\Lambda nl} = E_{\Lambda}^{lep} + E_{\Lambda nl}^{rad} + E_{\Lambda nl}^{rot}$. Here $E_{\Lambda}^{lep} = E_{\Lambda}(\infty)$ denotes the leptonic energy, $E_{\Lambda}(R)$ is defined by Eq. (6), and $E_{\Lambda nl}^{rad}$ is obtained by solving the radial equation with $l=0$, while the value of $E_{\Lambda nl}^{rot}$ is provided by the centrifugal term $l(l+1)/R^2$ in Eq. (15). The sequence of the energy scales for the quasibound molecular states with principal quantum number $n \gg 1$ recalls the energy scaling for normal diatomics: $E_{\Lambda}^{lep} \gg E_{\Lambda nl}^{rad} \gg E_{\Lambda nl}^{rot}$. In what follows concerning the quasimolecu-

TABLE I. The interaction energies $E_\Lambda(R)$ as a function of the internuclear distance R calculated for the values of leptonic orbital angular momentum projection $\Lambda=0$, 1, 2, 6, 30 (in atomic units).

R	$E_0(R)$	$E_1(R)$	$E_2(R)$	$E_6(R)$	$E_{30}(R)$
0.750	−1.58331	−1.58331	−1.58331	−1.58317	−1.58294
0.800	−1.50128	−1.49993	−1.49993	−1.49983	−1.49978
0.900	−1.37068	−1.36104	−1.36104	−1.36094	−1.35856
1.000	−1.27437	−1.24993	−1.24993	−1.24982	−1.24745
1.100	−1.20316	−1.15902	−1.15902	−1.15891	−0.91299
1.200	−1.15044	−1.08326	−1.08326	−1.08315	−0.84155
1.300	−1.11138	−1.01916	−1.01916	−1.01904	−0.78374
1.400	−1.08242	−0.96422	−0.96422	−0.96410	−0.73683
1.500	−1.06095	−0.91658	−0.91658	−0.91648	−0.69864
1.600	−1.04503	−0.87493	−0.87493	−0.87481	−0.66743
1.700	−1.03325	−0.83817	−0.83817	−0.83805	−0.64182
1.800	−1.02454	−0.80549	−0.80549	−0.63034	−0.62070
1.900	−1.01811	−0.77625	−0.77625	−0.61285	−0.60320
2.000	−1.01338	−0.74993	−0.74993	−0.59829	−0.58864
2.200	−1.00736	−0.71385	−0.70448	−0.57584	−0.56625
2.500	−1.00323	−0.68478	−0.64993	−0.55374	−0.54410
3.000	−1.00133	−0.65920	−0.58071	−0.53365	−0.52400
3.500	−1.00099	−0.64643	−0.56967	−0.52373	−0.51408
4.000	−1.000832	−0.639326	−0.564065	−0.518470	−0.508809
5.000	−1.000465	−0.632243	−0.559105	−0.513732	−0.504065
7.000	−1.0000833	−0.627372	−0.556435	−0.511135	−0.501464
10.000	−1.0000043	−0.625650	−0.555725	−0.510418	−0.500745
15.000	−0.9999969	−0.625167	−0.555571	−0.510233	−0.500562
20.000	−0.9999964	−0.625066	−0.555552	−0.510203	−0.500517

lar levels the quantum numbers $\Lambda$and l are supposed to be fixed.

The leptonic potentials $V_\Lambda^{lep}(R)$, the energies $E_{\Lambda nl}$, and the corresponding wave functions completely describe the $H\bar{H}^*$ quasimolecule and have been employed in calculations of observables characterizing the $H\bar{H}^*$ system, such as the decay rates for different processes.

III. POTENTIAL ENERGY CURVES

Results for the $H\bar{H}^*$ interaction energies $E_\Lambda(R)$ as a functions of R defined in Eq. (6) are presented in Table I for the values of leptonic orbital angular momentum projection $\Lambda=0,1,2,6,30$. All potential energy curves decrease monotonically as the internuclear distance R decreases. Values of the ground-state energy $E_0(R)$ are in close agreement with those of earlier calculations [5]. At large internuclear distances the behavior of $E_\Lambda(R)$ can be evaluated pertubatively. In case of $\Lambda=0$ the expression $E_0(R)\approx -C_6/R^6$ describes the dispersion interaction of the H and $\bar{H}$ atoms in their ground states. The variational calculation [5] gives the value $C_6=6.5$ in agreement with the result for the H_2 molecule [22]. In principle, the behavior of all the curves $E_\Lambda(R)$ for $R\to\infty$ should be the same as for H_2 molecule: the influence of the symmetry properties of the homonuclear H_2 molecule on the behavior of $E_\Lambda(R)$ curves at large R values appears to be the same as the influence of the charge conjugation symmetry in the $H\bar{H}$ system. For the first excited state the expression $E_1(R)\approx -C_3/R^3-C_6/R^6$ with $C_3=0.555$ and $C_6=146$ approximates well the function $E_1(R)$ obtained variationally in our calculations. The same calculation for $\Lambda=2$ yields $E_2(R)\approx -C_5/R^5-C_6/R^6$ with $C_5=0.6$ and $C_6=790$. The values of C_6 for $\Lambda=1$ and $\Lambda=2$ were estimated employing the well-known London formula $C_6=\frac{3I_HI_{\bar{H}}}{2(I_H+I_{\bar{H}})}\alpha_H\alpha_{\bar{H}}$ with ionization potentials (I) and static polarizabilities (α) for the H and $\bar{H}$ atoms in the corresponding states [see Eq. (5)]. The polarizabilities α were calculated for different states of the hydrogen atom employing a method described in [23]. The values of α increase rapidly for excited states of H atom and lead to large values of coefficients C_6 for the $H\bar{H}^*$ system with nonzero Λ. However, the dispersion formula approximates well the interatomic interaction energy if the overlap between charge densities of both atoms is negligible. Therefore it cannot be applied for a description of the potential curves corresponding to high values of $\Lambda=6,30$ at internuclear distances $R\leqslant 20$ a.u. Note that the overlap between H and $\bar{H}$ charge densities does not change significantly the density distributions of the H and $\bar{H}$ atoms at $R\sim 20$ a.u. due to the properties of the corresponding states and the asymptotic for-

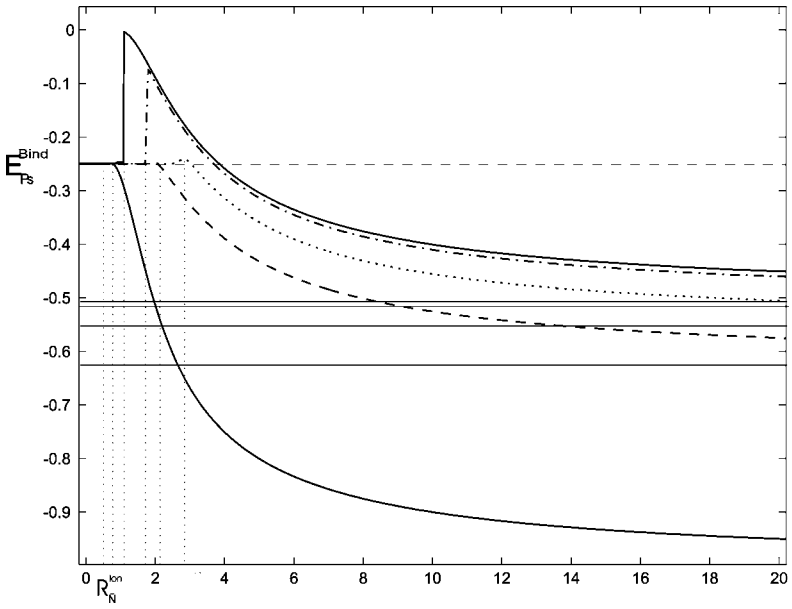

FIG. 1. The leptonic potentials for the ground state ($\Lambda=0$) and for excited states ($\Lambda=1,2,6,30$), $V_0^{lep}(R)$ (solid line), $V_1^{lep}(R)$ (dashed line), $V_2^{lep}(R)$ (dotted line), $V_6^{lep}(R)$ (dash-dotted line), and $V_{30}^{lep}(R)$ (solid line). The potentials are plotted as functions of the internuclear distance R (in atomic units). The energies of the noninteracting $H+\bar{H}^*$ system are indicated by solid straight lines parallel to the horizontal axis; for $\Lambda=0$ this line coincides with the abscissa axis. The vertical dotted lines indicate the critical distances $R_c(\Lambda)$.

mula (5) still holds. The behavior of the potential curves with $\Lambda=6,30$ was extrapolated beyond $R=20$ a.u. so that the curves smoothly reach their asymptotic energies of two noninteracting atoms. Calculated values of decay rates do not depend on the way $E_\Lambda(R)$ were extrapolated.

The ECG orbitals describe correctly the system of a Ps atom interacting weakly with the p^-p^+ pair, which is demonstrated by the behavior of leptonic potentials $V_\Lambda^{lep}(R)$ depicted in Fig. 1. For internuclear distances smaller than the critical value $R_c(\Lambda)$ the function $V_\Lambda^{lep}(R)$ approaches the ground-state energy of the Ps atom, $E_{Ps}^{bind}=-0.25$ a.u. The values of the critical distances $R_c(\Lambda)$ and nonadiabatic corrections near $R_c(\Lambda)$ are compiled in Table II for $\Lambda=0,1,2,6,30$. The characteristics of the potential energy curve for the ground state and the origin of the critical distance $R_c(0)$ have been discussed in [9]. As has been pointed out in [9] the energy curve $E_0(R)$ coincides with the interaction energy between H and $\bar{H}$ atoms, $E_{H\bar{H}}(R)$, for $R\geqslant R_c(0)$ and with the energy of weakly interacting Ps and Pt atoms, $E_{Ps+Pt}(R)\sim -1/R-0.25$, for $R\leqslant R_c(0)$. The same situation occurs for excited leptonic states of the $H\bar{H}^*$ system (see Fig. 1). For the internuclear distances $R\geqslant R_c(\Lambda)$ the wave function $\Psi_\Lambda^{lep}(\vec{r}_{e^-},\vec{r}_{e^+},\vec{R})$ describes the interaction between H and $\bar{H}^*$ atoms with nuclei fixed at the distance R. For the internuclear distances $R\leqslant R_c(\Lambda)$ the function $\Psi_\Lambda^{lep}(\vec{r}_{e^-},\vec{r}_{e^+},\vec{R})$ describes the ground state of the Ps atom, moving in the field of the p^-p^+ pair, with the angular momentum projection Λ, since the orbital state of light particles cannot change within the Born-Oppenheimer approximation. Thus the energy of the Ps atom in the p^-p^+ center-of-mass frame consists of two parts: $E_{Ps}=E_{Ps}^{bind}+E_{Ps}^{rot}$ with $E_{Ps}^{rot}=\frac{\Lambda^2}{2I_{Ps}}$. Here $I_{Ps}=2\rho_{Ps}^2$ is the moment of inertia of the Ps atom with respect to the internuclear axis and ρ_{Ps} denotes the average distance between center of mass of the Ps atom and molecular axis. Near the critical point $R_c(\Lambda)$ the value of $E_{Ps+Pt}\sim E_{Ps}-1/R$ becomes smaller than $E_\Lambda(R)$ and $H\bar{H}^*$ transforms into the Ps+Pt system.

TABLE II. The nonadiabatic corrections $\Delta V_\Lambda^{lep}(R_c(\Lambda))$ and internuclear critical distances $R_c(\Lambda)$ calculated for the different leptonic orbital angular momentum projections $\Lambda=0$, 1, 2, 6, 30 (in atomic units).

Λ	0	1	2	6	30
$R_c(\Lambda)$	0.752	2.07	3.03	1.79	1.08
$\Delta V_\Lambda^{lep}(R_c(\Lambda))$	0.24	0.5	1.0	6.9	9.0

The density distributions for the electron and the positron in the $H\bar{H}^*$ system in the states with nonzero but small values of Λ overlap at larger internuclear distances R that for $\Lambda=0$ (ground state). Accordingly, the critical distance $R_c(\Lambda)$, where the $H\bar{H}^*$ system transforms into Ps and Pt atoms, increases as Λ increases for small values of leptonic orbital angular momentum projection (see Table II). For a low Λ the value of the rotational part of the Ps energy E_{Ps}^{rot} is small compared to the absolute value of E_{Ps}^{bind}. So the energy of the Ps atom is approximately its binding energy. Thus, when the leptonic potential corresponding to $\Lambda=1$, 2 reaches the value of E_{Ps}^{bind}, the $H+H^*$ system decays into separate Ps and Pt atoms, as it was in case of $\Lambda=0$ (see Fig. 1).

The $H\bar{H}^*$ system with high values of Λ can be considered as an ion $(H\bar{H})^-$ (i.e., $p\bar{p}e^-$ system) and the positron e^+ weakly bound to this ion. As the value of Λ increases $R_c(\Lambda)$ decreases and in the limit $\Lambda\to\infty$ it should approach the value of the internuclear critical distance $R_c^{ion}=0.639a_0$ for the ion $(H\bar{H})^-$ [24] (see Fig. 1). The rotational energy E_{Ps}^{rot} corresponding to the state with high Λ becomes essential compared to E_{Ps}^{bind}. Therefore $V_\Lambda^{lep}(R)$ reaches the higher energy values than in case of low Λ (see Fig. 1). After the decay of the $H\bar{H}^*$ system the electron and the positron are not bound to the p^-p^+ pair, so the Ps atom flies away rotating around the internuclear axis. The energy E_{Ps}^{rot} becomes negligible since the value of ρ_{Ps} becomes infinite and the leptonic potentials

TABLE III. Numerical results for the annihilation rates $\Gamma_{2\gamma}^{e^-e^+}$, $\Gamma^{p^-p^+}$ and for the decay rate Γ^{Ps+Pt} for hadronic quantum numbers $n=19-26$, $l=0,1$, and $\Lambda=0$.

n	$\Gamma_{2\gamma}^{e^-e^+}$(GHz)		$\Gamma^{p^-p^+}$(GHz)	Γ^{Ps+Pt}(GHz)	
	$l=0$	$l=1$	$l=0$	$l=0$	$l=1$
19	1.298	1.268	3.2×10^6	2.9×10^6	2.5×10^6
20	3.641	3.621	2.7×10^6	5.0×10^5	4.3×10^5
21	3.847	3.843	2.2×10^6	3.3×10^5	2.7×10^5
22	4.511	4.512	1.8×10^6	1.5×10^5	1.2×10^5
23	4.602	4.596	1.4×10^6	9.0×10^4	7.2×10^4
24	4.499	4.497	1.1×10^6	5.3×10^4	2.2×10^4
25	4.303	4.305	8.2×10^5	2.7×10^4	1.9×10^4
26	3.861	3.864	5.4×10^5	1.1×10^4	6.9×10^3

$V_\Lambda^{lep}(R)$ corresponding to the high values of Λ dive down to the value of the ground-state binding energy of the Ps atom E_{Ps}^{bind} (see Fig. 1).

IV. DECAY CHANNEL $H\bar{H}^* \rightarrow Ps+Pt$

In [9] the decay rates for the process $H\bar{H}\rightarrow Ps+Pt$ have been estimated applying a semiclassical approach for the description of the hadronic motion. A similar estimate can be made for the process $H\bar{H}^*\rightarrow Ps+Pt$. According, hadronic states with high principal quantum numbers $n\gg1$ should be considered. For such states the probability of finding the proton and antiproton at the internuclear distances $R\geqslant R_c(\Lambda)$, where the $H\bar{H}^*$ system may still exist, will be essential. This probability is equal to

$$P_{\Lambda nl}=\int_{R_c(\Lambda)}^{\infty}|\chi_{\Lambda nl}(R)|^2dR. \tag{16}$$

Within this semiclassical picture the decay rate for the process $H\bar{H}^*\rightarrow Ps+Pt$ can be estimated via [9]

TABLE IV. Numerical results for the annihilation rates $\Gamma_{2\gamma}^{e^-e^+}$, $\Gamma^{p^-p^+}$ and for the decay rate Γ^{Ps+Pt} for hadronic quantum numbers $n=33-42$, $l=0,1$, and $\Lambda=1$.

n	$\Gamma_{2\gamma}^{e^-e^+}$(GHz)		$\Gamma^{p^-p^+}$(GHz)	Γ^{Ps+Pt}(GHz)	
	$l=0$	$l=1$	$l=0$	$l=0$	$l=1$
33	1.178	1.169	5.5×10^5	1.5×10^5	1.1×10^5
34	1.687	1.670	4.3×10^5	6.1×10^4	4.8×10^4
35	0.734	0.738	3.2×10^5	2.7×10^4	2.0×10^4
36	1.032	1.031	2.5×10^5	1.5×10^4	1.1×10^4
37	0.934	0.934	1.9×10^5	7.9×10^3	5.7×10^3
38	0.632	0.631	1.4×10^5	3.8×10^3	2.7×10^3
39	0.585	0.585	9.5×10^4	1.8×10^3	1.2×10^3
40	0.388	0.387	6.5×10^4	8.1×10^2	5.5×10^2
41	0.243	0.243	4.3×10^4	3.5×10^2	2.1×10^2
42	0.153	0.153	2.6×10^4	1.3×10^2	7.1×10^1

TABLE V. Numerical results for the annihilation rates $\Gamma_{2\gamma}^{e^-e^+}$, $\Gamma^{p^-p^+}$ and for the decay rate Γ^{Ps+Pt} for hadronic quantum numbers $n=38-41$, $l=0,1$, and $\Lambda=2$.

n	$\Gamma_{2\gamma}^{e^-e^+}$(GHz)		$\Gamma^{p^-p^+}$(GHz)	Γ^{Ps+Pt}(GHz)	
	$l=0$	$l=1$	$l=0$	$l=0$	$l=1$
38	0.620	0.617	2.1×10^5	4.7×10^4	2.4×10^4
39	0.398	0.399	1.4×10^5	1.2×10^4	7.6×10^3
40	0.284	0.285	8.1×10^4	3.1×10^3	1.7×10^3
41	0.196	0.196	4.0×10^4	4.6×10^2	3.4×10^2

$$\Gamma_{\Lambda nl}^{Ps+Pt}=\frac{1}{\tau_{\Lambda nl}}\sim2\frac{|\Delta E_{\Lambda nl}|}{\pi}\frac{1-P_{\Lambda nl}}{P_{\Lambda nl}}. \tag{17}$$

Here $\tau_{\Lambda nl}$ is the semiclassical lifetime of the unstable quasimolecular state $|\Lambda nl\rangle$ and $\Delta E_{\Lambda nl}$ is the difference between two neighboring levels, one of which has the quantum numbers n,l and depends weakly on these quantum numbers if $n\gg1$. The expression $P_{\Lambda nl}/(1-P_{\Lambda nl})$ represents the relative probability for finding the particles p^- and p^+ at a distance $R\geqslant R_c(\Lambda)$. Values of $\Gamma_{\Lambda nl}^{Ps+Pt}$ for $\Lambda=0,1,2,6,30$ and $l=0,1$ are compiled in Tables III–VII together with the e^-e^+ and p^-p^+ annihilation decay rates.

The formation of the quasimolecular levels with different n,l values requires special consideration. The necessary condition for such a formation is

$$T_{\Lambda nl}\ll t_{int}, \tag{18}$$

where $T_{\Lambda nl}=2\pi/|\Delta E_{\Lambda nl}|$ denotes the semiclassical period for the considered quasimolecular level and t_{int} is the interaction time during the formation process of $H\bar{H}^*$ quasimolecule. This time can be estimated via

$$t_{int}=\frac{s}{v}, \tag{19}$$

where s is the characteristic length of the process and v is the relative velocity of ultracold hadrons. It is assumed that $s\approx10$ a.u. $\approx10^{-7}$ cm for low values of Λ and $s\gg10^{-7}$ cm for Rydberg leptonic states. Under the experimental conditions [1–3] the relative velocity is estimated as $v\approx10^3$ cm/s. For

TABLE VI. Numerical results for the annihilation rate $\Gamma^{p^-p^+}$ and for the decay rate Γ^{Ps+Pt} for hadronic quantum numbers $n=36-41$, $l=0,1$, and $\Lambda=6$.

n	$\Gamma^{p^-p^+}$(GHz)	Γ^{Ps+Pt}(GHz)	
	$l=0$	$l=0$	$l=1$
36	5.1×10^5	2.7×10^4	2.2×10^4
37	2.1×10^5	7.0×10^3	4.9×10^3
38	1.2×10^5	2.7×10^3	1.6×10^3
39	7.2×10^4	1.0×10^3	6.1×10^2
40	4.4×10^4	3.7×10^2	2.0×10^2
41	2.1×10^4	8.3×10^1	4.4×10^1

TABLE VII. Numerical results for the annihilation rate $\Gamma^{p^-p^+}$ and for the decay rate Γ^{Ps+Pt} for hadronic quantum numbers $n=27-36$, $l=0,1$, and $\Lambda=30$.

n	$\Gamma^{p^-p^+}$(GHz)	Γ^{Ps+Pt}(GHz)	
	$l=0$	$l=0$	$l=1$
27	1.5×10^6	1.6×10^5	1.3×10^5
28	1.0×10^6	7.4×10^4	6.5×10^4
29	8.0×10^5	3.3×10^4	3.5×10^4
30	7.2×10^5	2.9×10^4	2.3×10^4
31	5.8×10^5	1.8×10^4	1.5×10^4
32	4.5×10^5	1.1×10^4	8.6×10^3
33	3.4×10^5	6.3×10^3	4.8×10^3
34	2.5×10^5	3.4×10^3	2.5×10^3
35	1.8×10^5	1.7×10^3	1.2×10^3
36	1.2×10^5	7.9×10^2	4.4×10^2

low values of Λ the interaction time $t_{int}\approx10^{-10}$ s should be compared with $T_{\Lambda nl}\approx10^{-12}$ s for $\Lambda=0$, $n=23$, $l=1$. Thus the inequality (18) holds in this case [9]. For high values of Λ the numerical calculation gives $T_{\Lambda nl}\approx2\times10^{-10}$ s ($\Lambda=30$, $n=30$, $l=1$), but the interaction time also becomes larger $t_{int}\gg10^{-10}$ s. So we conclude that the quasimolecular Rydberg states also should arise in the experimental situation described in [1–3].

V. e^-e^+ AND p^-p^+ ANNIHILATION

The annihilation rate of a pointlike particle and antiparticle separated by the distance $\vec{r}$ is proportional to the matrix element of the spatial delta function $\delta(\vec{r})$. The proportionality factor—i.e., the so-called annihilation constant—is obtained as the number of annihilation events per unit density and unit time. The following consideration concerning leptons will focus on the two-photon (2γ) annihilation of electrons and positrons with total spin $S=0$, since the triplet state annihilates into three photons with smaller probability. The spin-averaged 2γ-annihilation constant for the electron-positron pair is equal to $A_{2\gamma}^{e^-e^+}=4\pi c r_{e^-}^2\approx2\times10^{11}$ Hz [13], where $r_{e^-}=\frac{e^2}{mc^2}$ is the electrostatic radius of electron. The 3γ-annihilation constant is much smaller, $A_{3\gamma}^{e^-e^+}\approx2\times10^8$ Hz. As in Refs. [9,12] the value for the p^-p^+ annihilation constant, $A^{p^-p^+}\approx7\times10^9$ Hz, was taken from the experiment [25], which also account for various other p^-p^+-annihilation channels, such as, e.g., $p^-p^+\to\pi^0\pi^0$, $p^-p^+\to\pi^-\pi^+$, etc.

The expression for the leptonic 2γ-annihilation rate within the $H\bar{H}$ system reads

$$\Gamma_{2\gamma}^{e^-e^+}=A_{2\gamma}^{e^-e^+}\langle\Psi(\vec{r}_{e^-},\vec{r}_{e^+},\vec{R})|\delta(\vec{r}_{e^-}-\vec{r}_{e^+})|\Psi(\vec{r}_{e^-},\vec{r}_{e^+},\vec{R})\rangle, \tag{20}$$

where $\Psi(\vec{r}_{e^-},\vec{r}_{e^+},\vec{R})$ denotes the total wave function defined in Eq. (1). According to Eqs. (1) and (15), $\Gamma_{2\gamma}^{e^-e^+}$ can be written in the form

$$\Gamma_{2\gamma}^{e^-e^+}=A_{2\gamma}^{e^-e^+}\int_{R_c(\Lambda)}^{\infty}|\chi_{\Lambda nl}(R)|^2P_\Lambda(R)dR, \tag{21}$$

where $P_\Lambda(R)$ is the e^-e^+-coalescence probability distribution [9,13]:

$$P_\Lambda(R)=\langle\Psi_\Lambda^{lep}(\vec{r}_{e^-},\vec{r}_{e^+},\vec{R})|\delta(\vec{r}_{e^-}-\vec{r}_{e^+})|\Psi_\Lambda^{lep}(\vec{r}_{e^-},\vec{r}_{e^+},\vec{R})\rangle. \tag{22}$$

In Eq. (21) the integration over internuclear distances R extends from the lower bound $R_c(\Lambda)$ up to infinity since

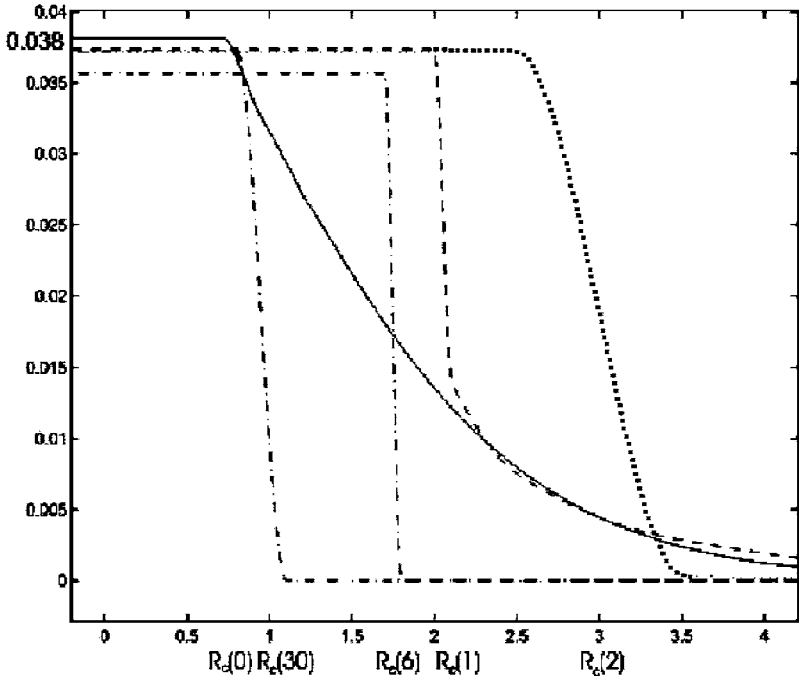

FIG. 2. The coalescence probability distributions $P_0(R)$ (solid line), $P_1(R)$ (dashed line), $P_2(R)$ (dotted line), $P_6(R)$, and $P_{30}(R)$ (dash-dotted line) are plotted as a function of the internuclear distance R (in atomic units).

contributions to the annihilation rate arise only from distances where the $H\bar{H}^*$ quasimolecule still exists. The e^-e^+-coalescence probability distributions $P_\Lambda(R)$ for $\Lambda=0,1,2,6,30$ are depicted in Fig. 2. As can be seen from Fig. 2, $P_\Lambda(R)$ tends to zero quite rapidly for distances $R \geqslant R_c(\Lambda)$, in particular for Rydberg states $\Lambda=6,30$. Hence the leptonic annihilation decay rates for these quasimolecular states are close to zero. This follows from the small overlap of the electron and positron density distributions in the Rydberg states of the $H\bar{H}^*$ quasimolecule.

For distances $R \leqslant R_c(\Lambda)$ all the functions $P_\Lambda(R)$ approach the constant value $P_\Lambda(0) \approx |\psi^{Ps}_{100}(0)|^2 = \frac{1}{8\pi}$, which corresponds to the coalescence probability in free positronium. The behavior of $P_\Lambda(R)$ confirms the fact that all considered excited leptonic states of the $H\bar{H}^*$ system decay into the Ps atom in the ground state and Pt atom. The expression for the p^-p^+-annihilation rate can be obtained similarly using the hadronic part of the wave function $\Psi^{had}_{\Lambda nlm}$ [see Eq. (14)]:

$$\Gamma^{p^-p^+} = A^{p^-p^+} \left| \frac{\chi_{\Lambda nl}(R)}{R} \right|^2_{R\to 0}, \tag{23}$$

with $\chi_{\Lambda nl}(R)$ calculated by solving Eq. (15). For $l \neq 0$, $\Gamma^{p^-p^+} \approx 0$, since the radial part of the hadronic wave function $\chi_{\Lambda nl}(R)$ behaves like $\sim R^{l+1}$ in the limit $R \to 0$. The P states contribute to the $\Gamma^{p^-p^+}$ at high energies (see, for example, [26–28]). However, the $H\bar{H}^*$ system in experiments [1–3] is obtained with ultracold atoms so that at low energies Eq. (23) holds [12]. Numerical results for the annihilation decay rates $\Gamma^{e^-e^+}_{2\gamma}$ and $\Gamma^{p^-p^+}$ together with the $H\bar{H}^* \to Ps+Pt$ decay rates are presented in Tables III–VII for the quasimolecular states with quantum numbers $\Lambda=0,1,2,6,30$ and $l=0,1$.

The higher hadronic quasibound states are considered since only for these states does the probability to find the proton and antiproton at distances larger than the critical one become essential; i.e., the quasibound system exists during a considerable time period. An upper bound for the number N of such quasibound states is determined by the particular properties of the potential curve $E_\Lambda(R)$. The quasimolecular leptonic state with $\Lambda=1$ requires one to take into account the largest number of hadronic Rydberg states since the corresponding interaction energy between H and $\bar{H}^*$ decreases only as $1/R^3$ while for the other leptonic levels the interaction energy decreases faster.

VI. CONCLUSIONS

Concluding we can state that the generalized ECG basis set is suitable for describing the interaction between H and $\bar{H}$ atoms in an arbitrary leptonic state with high precision. This has been confirmed within this paper by checking the obtained results at large and small internuclear distances R and by making a comparison with other investigations of the ground state of the $H\bar{H}$ system. The advantage of the present description is that it can be generalized to the case of an arbitrary two-center Coulomb system with N electrons and positrons. In particular, the atom-antiatom interaction can be described in effective core approximation employing generalized ECG basis sets.

On the other hand, the investigation of the $H\bar{H}^*$ system is more close to the experimental situation, since up to now in experiments [1–3] the $\bar{H}^*$ atoms have been produced only in Rydberg states. In the present paper observable properties of $H\bar{H}^*$ quasimolecule, such as decay rates for different processes, have been calculated.

The role of the decay processes in the $H\bar{H}^*$ system involving excited leptonic states is the same as for the $H\bar{H}$ ground state. However, in the case of excited leptonic states the numerical results for the decay rates are smaller than the corresponding ones in the $H\bar{H}$ ground state since in the former case the particles are at larger distances. This may be considered as a hint for the creation of metastable quasibound states of matter and antimatter in the future. From this point of view experimental investigations of the properties of atom-antiatom quasimolecules in Rydberg state are more favorable than to study their ground-state properties: unlike normal molecules the atom-antiatom quasimolecules in Rydberg states are more stable than in the ground state.

ACKNOWLEDGMENTS

The authors are also grateful to I. I. Tupitsyn, M. G. Kozlov, and A. V. Titov for valuable discussions. This work was supported by INTAS Grant No. 0354-3604 and by DFG. V.S. and L.L. are grateful to the TU Dresden for the hospitality during their visit in 2004 and 2005 and acknowledge financial support from DAAD, DFG, and MPI. The work of V.S. and L.L. was also supported by RFBR Grant No. 02-02-16578. V.S. acknowledges support by the nonprofit foundation "Dynasty" (Moscow). G.P. acknowledges financial support from BMBF, DFG, and GSI.

APPENDIX: EXPRESSIONS FOR MATRIX ELEMENTS

This appendix provides explicit expressions for the overlap integral between leptonic wave functions involving two Gaussians multiplied by a spherical harmonic [Eqs. (11) and (12)] and the corresponding matrix elements for all terms appearing in the leptonic Hamiltonian (3) as well as for the spatial delta function $\delta(\vec{r}_{e^-} - \vec{r}_{e^+})$.

Due to the symmetry of the $H\bar{H}$ system, the leptonic wave function is invariant under rotations around the internuclear axis $\vec{R}$. This condition reduces the number of variational parameters so that $\vec{R}^{e^-}_i = (0,0,R^{e^-}_i)$ and $\vec{R}^{e^+}_i = (0,0,R^{e^+}_i)$, respectively. It is further convenient to define the parameters $\delta^{e^-}_i = R/2 + R^{e^-}_i$ and $\delta^{e^+}_i = R/2 - R^{e^+}_i$ [see Eq. (11)], which in the asymptotic limit $R \to \infty$ yield $\Psi^{lep}(\vec{r}_{e^-}, \vec{r}_{e^+}, \vec{R}) = \Psi_H(\vec{r}_{e^-} + \vec{R}/2)\Psi_{\bar{H}}(\vec{r}_{e^+} - \vec{R}/2)$ and $\delta^{e^\pm}_i \to 0$, respectively. The basis functions $\psi_i = \langle \vec{r}_{e^-}\vec{r}_{e^+} | a_i b_i c_i \delta^{e^-}_i \delta^{e^+}_i u^{e^-}_i u^{e^+}_i \rangle$ depend on seven parameters. Expressions for $\langle \psi_i | \psi_j \rangle$, $\langle \psi_i | \hat{T} | \psi_j \rangle$, and $\langle \psi_i | \hat{U} | \psi_j \rangle$, where $\hat{T}$ and $\hat{U}$ are the kinetic and potential energy operators in the Hamiltonian (3) and $\langle \psi_i | \delta(\vec{r}_{e^-} - \vec{r}_{e^+}) | \psi_j \rangle$, are given be-

low. For the non-normalized Gaussians ψ_i, ψ_j the overlap integral is equal to

$$\langle a_i b_i c_i \delta_i^{e^-} \delta_i^{e^+} u_i^{e^-} u_i^{e^+} | a_j b_j c_j \delta_j^{e^-} \delta_j^{e^+} u_j^{e^-} u_j^{e^+} \rangle = \langle \psi_i | \psi_j \rangle = \frac{\pi^3}{\sigma^{3/2}} q^\Lambda \frac{(2\Lambda+1)!!}{4\pi} \times \exp\left(-\frac{abc}{\sigma}(R-\beta-\gamma)^2 - \frac{b_i b_j}{b}\delta_{e^-}^2 - \frac{c_i c_j}{c}\delta_{e^+}^2 \right). \tag{A1}$$

In the above expression the notations $a=a_i+a_j$, $b=b_i+b_j$, $c=c_i+c_j$, $\sigma=ab+bc+ca$, $\beta=(b_i\delta_i^{e^-}+b_j\delta_j^{e^-})/b$, $\gamma=(c_i\delta_i^{e^+}+c_j\delta_j^{e^+})/c$, $\delta_{e^-}=\delta_i^{e^-}-\delta_j^{e^-}$, $\delta_{e^+}=\delta_i^{e^+}-\delta_j^{e^+}$, and $q=(a(u_i^{e^-}+u_i^{e^+})\times(u_j^{e^-}+u_j^{e^+})+cu_i^{e^-}u_j^{e^-}+bu_i^{e^+}u_j^{e^+})/(2\sigma)$ are introduced. All matrix elements are expressed in terms of $\langle\psi_i|\psi_j\rangle$, and then the functions ψ_i are redefined so that $\langle\psi_i|\psi_i\rangle=1$ holds. To represent the matrix elements in a compact form the following functions of variational parameters are defined: $f=R-\beta-\gamma$, $\rho_{e^-}=-\frac{ac}{\sigma}f-\beta$, $\rho_{e^+}=-\frac{ab}{\sigma}f-\gamma$, $\delta_{ab}=a_ib_j-b_ia_j$, and $\sigma_{ij}=a_ib_j+b_jc_i+c_ia_j$,

$$S=\frac{3}{\sigma}[a(b_ib_j+c_ic_j)+a_ia_j(b+c)+c(a_i+b_i)(a_j+b_j)+b(a_i+c_i)(a_j+c_j)],$$

$$P=\frac{2}{\sigma}[\delta_{ab}^2c^2+\delta_{ac}^2b^2],$$

$$Q=\frac{(\sigma_{jj}+\sigma_{ij})(\sigma_{ii}+\sigma_{ji})-\delta_{ac}^2}{\sigma^2}u_i^{e^-}u_j^{e^-}+\frac{(\sigma_{ii}+\sigma_{ij})(\sigma_{jj}+\sigma_{ji})-\delta_{ab}^2}{\sigma^2}u_i^{e^+}u_j^{e^+}+\frac{\delta_{ab}(\sigma_{ii}+\sigma_{ji})+\delta_{ca}(\sigma_{jj}+\sigma_{ji})}{\sigma^2}u_i^{e^+}u_j^{e^-}+\frac{\delta_{ba}(\sigma_{jj}+\sigma_{ij})+\delta_{ac}(\sigma_{ii}+\sigma_{ij})}{\sigma^2}u_i^{e^-}u_j^{e^+}.$$

Accordingly, the matrix elements, expressed in terms of these functions, read

$$\langle\psi_i|\hat{T}|\psi_j\rangle=\left[S-PR^2+\Lambda\frac{Q}{q}\right]\langle\psi_i|\psi_j\rangle, \tag{A2}$$

$$\left\langle\psi_i\left|\frac{1}{\left|\vec{r}_{e^-}+\frac{1}{2}\vec{R}\right|}\right|\psi_j\right\rangle=2\sqrt{\frac{\sigma}{\pi(a+c)}}F_\Lambda\left(\alpha_{e-},\beta_{e-};\frac{\sigma\rho_{e^-}^2}{a+c}\right)\times\langle\psi_i|\psi_j\rangle, \tag{A3}$$

$$\alpha_{e-}=\frac{u_i^{e^+}u_j^{e^+}}{2(a+c)q}, \tag{A3a}$$

$$\beta_{e-}=\frac{[a(u_j^{e^-}+u_j^{e^+})+cu_j^{e^-}][a(u_i^{e^-}+u_i^{e^+})+cu_i^{e^-}]}{2\sigma(a+c)q}, \tag{A3b}$$

$$\left\langle\psi_i\left|\frac{1}{\left|\vec{r}_{e^-}-\frac{1}{2}\vec{R}\right|}\right|\psi_j\right\rangle=2\sqrt{\frac{\sigma}{\pi(a+c)}}\times F_\Lambda\left(\alpha_{e-},\beta_{e-};\frac{\sigma(\rho_{e^-}+R)^2}{a+c}\right)\langle\psi_i|\psi_j\rangle, \tag{A4}$$

$$\left\langle\psi_i\left|\frac{1}{\left|\vec{r}_{e^+}-\frac{1}{2}\vec{R}\right|}\right|\psi_j\right\rangle=2\sqrt{\frac{\sigma}{\pi(a+b)}}F_\Lambda\left(\alpha_{e+},\beta_{e+};\frac{\sigma\rho_{e^+}^2}{a+b}\right)\times\langle\psi_i|\psi_j\rangle, \tag{A5}$$

$$\alpha_{e+}=\frac{u_i^{e^-}u_j^{e^-}}{2(a+b)q}, \tag{A5a}$$

$$\beta_{e+}=\frac{[a(u_j^{e^-}+u_j^{e^+})+bu_j^{e^+}][a(u_i^{e^-}+u_i^{e^+})+bu_i^{e^+}]}{2\sigma(a+b)q}, \tag{A5b}$$

$$\left\langle\psi_i\left|\frac{1}{\left|\vec{r}_{e^+}+\frac{1}{2}\vec{R}\right|}\right|\psi_j\right\rangle=2\sqrt{\frac{\sigma}{\pi(a+b)}}\times F_\Lambda\left(\alpha_{e+},\beta_{e+};\frac{\sigma(\rho_{e^+}+R)^2}{a+b}\right)\langle\psi_i|\psi_j\rangle, \tag{A6}$$

$$\left\langle\psi_i\left|\frac{1}{|\vec{r}_{e^-}-\vec{r}_{e^+}|}\right|\psi_j\right\rangle=2\sqrt{\frac{\sigma}{\pi(b+c)}}F_\Lambda\left(\alpha_e,\beta_e;\frac{b^2c^2f^2}{\sigma(b+c)}\right)\times\langle\psi_i|\psi_j\rangle, \tag{A7}$$

$$\alpha_e=\frac{(u_i^{e^-}+u_i^{e^+})(u_j^{e^-}+u_j^{e^+})}{2(b+c)q}, \tag{A7a}$$

$$\beta_e=\frac{(cu_j^{e^-}-bu_j^{e^+})(cu_i^{e^-}-bu_i^{e^+})}{2\sigma(b+c)q}, \tag{A7b}$$

$$\langle\psi_i|\delta(\vec{r}_{e^-}-\vec{r}_{e^+})|\psi_j\rangle=\left(\frac{\sigma}{\pi(b+c)}\right)^{3/2}\alpha_e^\Lambda\exp\left(-\frac{b^2c^2f^2}{\sigma(b+c)}\right)\times\langle\psi_i|\psi_j\rangle. \tag{A8}$$

The function $F_\Lambda(\alpha,\beta;x)$ is defined by

$$F_\Lambda(\alpha,\beta;x)=\int_0^1[\alpha+\beta(1-s^2)]^\Lambda\exp(-xs^2)ds. \tag{A9}$$

[1] M. Amoretti *et al.*, Nature (London) **419**, 456 (2002).
[2] G. Gabrielse *et al.*, Phys. Rev. Lett. **89**, 213401 (2002).
[3] G. Gabrielse *et al.*, Phys. Rev. Lett. **89**, 233401 (2002).
[4] W. Kolos, D. L. Morgan, D. Schrader, and L. Wolniewicz, Phys. Rev. A **11**, 1792 (1975).
[5] K. Strasburger, J. Phys. B **35**, L435 (2002).
[6] K. Strasburger and H. Chojnacki, Phys. Rev. Lett. **88**, 163201 (2002).
[7] K. Strasburger, H. Chojnacki, and A. Sokolowska, J. Phys. B **38**, 3091 (2005).
[8] E. A. G. Armour and V. Zeman, Int. J. Quantum Chem. **74**, 645 (1999).
[9] L. Labzowsky, V. Sharipov, A. Prozorov, G. Plunien, and G. Soff, Phys. Rev. A **72**, 022513 (2005).
[10] S. Jonsell, A. Saenz, and P. Froelich, Nucl. Phys. A **663**, C959 (2000).
[11] P. Froelich, S. Jonsell, A. Saenz, B. Zygelman, and A. Dalgarno, Phys. Rev. Lett. **84**, 4577 (2000).
[12] S. Jonsell, A. Saenz, P. Froelich, B. Zygelman, and A. Dalgarno, Phys. Rev. A **64**, 052712 (2001).
[13] P. Froelich, S. Jonsell, A. Saenz, S. Eriksson, B. Zygelman, and A. Dalgarno, Phys. Rev. A **70**, 022509 (2004).
[14] B. Zygelman, A. Saenz, P. Froelich, and S. Jonsell, Phys. Rev. A **69**, 042715 (2004).
[15] K. Varga and Y. Suzuki, Phys. Rev. C **52**, 2885 (1995).
[16] Y. Suzuki, J. Usukura, and K. Varga, J. Phys. B **31**, 3465 (1998).
[17] K. Strasburger, J. Phys. B **37**, 4483 (2004).
[18] G. Ryzhikh and J. Mitroy, J. Phys. B **31**, 3465 (1998).
[19] G. G. Ryzhikh, J. Mitroy, and K. Varga, J. Phys. B **31**, 3965 (1998).
[20] W. R. Johnson, S. A. Blundell, and J. Sapirstein, Phys. Rev. A **37**, 307 (1988).
[21] C. Froese-Fischer and F. A. Parpia, Phys. Lett. A **179**, 198 (1993).
[22] L. D. Landau and E. M. Lifshitz, *Quantum Mechanics* (Pergamon, Oxford, 1977).
[23] M. I. Bhatti, K. D. Coleman, and W. F. Persen, Phys. Rev. A **68**, 044503 (2003).
[24] E. A. G. Armour, J. M. Carr, and V. Zeman, J. Phys. B **31**, L679 (1998).
[25] C. J. Batty *et al.*, Nucl. Phys. A **601**, 425 (1996).
[26] S. Devons *et al.*, Phys. Rev. Lett. **27**, 1614 (1971).
[27] M. Bargiotti *et al.*, Phys. Rev. D **65**, 012001 (2001).
[28] C. Amsler *et al.*, Phys. Rev. D **66**, 058101 (2002).